X-ray tests of the ATHENA mirror modules in BEaTriX: from design to reality

B. Salmaso, S. Basso, M. Ghigo, D. Spiga, G. Vecchi, et al.

B. Salmaso, S. Basso, M. Ghigo, D. Spiga, G. Vecchi, G. Sironi, V. Cotroneo, P. Conconi, E. Redaelli, A. Bianco, G. Pareschi, G. Tagliaferri, D. Sisana, C. Pelliciari, M. Fiorini, S. Incorvaia, M. Uslenghi, L. Paoletti, C. Ferrari, R. Lolli, A. Zappettini, M. Sanchez del Rio, G. Parodi, V. Burwitz, S. Rukdee, G. Hartner, T. Müller, T. Schmidt, A. Langmeier, D. D. Ferreira, S. Massahi, N. C. Gellert, F. Christensen, M. Bavdaz, I. Ferreira, M. Collon, G. Vacanti, N. Barrière, "X-ray tests of the ATHENA mirror modules in BEaTriX: from design to reality," Proc. SPIE 12181, Space Telescopes and Instrumentation 2022: Ultraviolet to Gamma Ray, 121810W (31 August 2022); doi: 10.1117/12.2628227

SPIE.

Event: SPIE Astronomical Telescopes + Instrumentation, 2022, Montréal, Québec, Canada

X-ray tests of the ATHENA mirror modules in BEaTriX: from design to reality

B. Salmaso[1a], S. Basso[a], M. Ghigo[a], D. Spiga[a], G. Vecchi[a], G. Sironi[a], V. Cotroneo[a], P. Conconi[a], E. Redaelli[a], A. Bianco[a], G. Pareschi[a], G. Tagliaferri[a], D. Sisana[b], C. Pelliciari[c], M. Fiorini[d], S. Incorvaia[d], M. Uslenghi[d], L. Paoletti[e], C. Ferrari[f], R. Lolli[f], A. Zappettini[f], M. Sanchez del Rio[g], G. Parodi[h], V. Burwitz[i], S. Rukdee[i], G. Hartner[i], T. Müller[i], T. Schmidt[i], A. Langmeier[i], D.D. Ferreira[l], S. Massahi[l], N.C. Gellert[l], F. Christensen[l], M. Bavdaz[m], I. Ferreira[m] M. Collon[n], G. Vacanti[n], N. Barrière[n]

[a]INAF Astronomical Observatory Brera, Via E. Bianchi 46, 23807 Merate, Lecco (Italy)
[b]Politecnico Milano Bovisa, Via La Masa 34, 20156 Milano (Italy)
[c]IIS Bachelet, Via Stignani 63/65, 20081 Abbiategrasso, Milano (Italy)
[d]INAF-IASF Milano, Via A. Corti 12, 40133 Milano (Italy)
[e]INAF Astronomical Observatory Padova, Vicolo Osservatorio 5, 35122 Padova (Italy)
[f]IMEM-CNR, Parco Area delle Scienze 37/A, 43124 Parma (Italy)
[g]European Synchrotron Radiation Facility, B.P. 220, 38043 Grenoble (France)
[h]BCV Progetti, Via S. Orsola 1, 20123 Milano (Italy)
[i]Max-Planck-Institut für extraterrestrische Physik, Giessenbachstr, 85748 Garching (Germany)
[l]DTU-space, Juliane Maries Vej 30, DK-2100 Copenhagen (Denmark)
[m]ESTEC, European Space Agency, Keplerlaan 1, 2201 AZ Noordwijk (Netherlands)
[n]cosine, Warmonderweg 14, 2171 AH Sassenheim, (The Netherlands)

ABSTRACT

The BEaTriX (Beam Expander Testing X-ray) facility is now operative at the INAF-Osservatorio Astronomico Brera (Merate, Italy). This facility has been specifically designed and built for the X-ray acceptance tests (PSF and Effective Area) of the ATHENA Silicon Pore Optics (SPO) Mirror Modules (MM). The unique setup creates a parallel, monochromatic, large X-ray beam, that fully illuminates the aperture of the MMs, generating an image at the ATHENA focal length of 12 m. This is made possible by a microfocus X-ray source followed by a chain of optical components (a paraboloidal mirror, 2 channel cut monochromators, and an asymmetric silicon crystal) able to expand the X-ray beam to a 6 cm × 17 cm size with a residual divergence of 1.5 arcsec (vertical) × 2.5 arcsec (horizontal). This paper reports the commissioning of the 4.5 keV beam line, and the first light obtained with a Mirror Module.

Keywords: BEaTriX, ATHENA, X-ray testing, X-ray microfocus source, beam expander, asymmetric diffraction, crystals, Silicon Pore Optics

1. INTRODUCTION

ATHENA is a Large-class mission in preparation by ESA with launch foreseen in 2030's. The mission is intended to study the hot and energetic universe by measuring the X-rays emitted by extremely hot sources [1]. The telescope will have an effective area of 1.4 m^2 and an angular resolution of 5 arcsec Half Energy Width (HEW) at 1 keV. The large effective area and the high resolution will permit to distinguish distant and faint objects often located in crowded fields, providing the breaking leap required to achieve the science goals of ATHENA. The large dimension of the telescope (diameter of 2.5 m) is reached with a modular approach, where the segments are manufactured individually and lately

[1] corresponding author: bianca.salmaso@inaf.it; phone +39-02-72320-428; www.brera.inaf.it

Space Telescopes and Instrumentation 2022: Ultraviolet to Gamma Ray, edited by Jan-Willem A. den Herder, Shouleh Nikzad, Kazuhiro Nakazawa, Proc. of SPIE Vol. 12181, 121810W · © 2022 SPIE · 0277-786X · doi: 10.1117/12.2628227

assembled with a hierarchical principle. The Silicon Pore Optics (SPO) technology was adopted to reach the requirements and to keep the mass under control. It is developed by cosine, ESA and its partners, both in academia and industry [2,3]. The starting material are super-polished silicon wafers, mainly produced for the semi-conductor industry, with a very low roughness that makes them ideal for reflecting X-rays. Dedicated robotic machines process the wafers into coated rectangular plates, bend and assemble them into the desired figure with stiffening ribs into X-ray Optical Units (XOUs). Four XOUs are then assembled into a Mirror Module (MM) with Wolter I geometry at the Physikalisch-Technische Bundesanstalt (PTB) laboratory of the BESSY-II synchrotron facility in Berlin [4]. To populate the entire telescope, 600 MMs need to be produced in the foreseen time of 2 years. A proper process control to support the production is needed, able to test all the MMs, with an X-ray beam, for acceptance before their integration. Ideally, a large parallel X-ray beam, as the one created by an astronomical object, is required but it is difficult to be obtained. Up to now, two alternative solutions were adopted.

Synchrotron light is used at XPBF 2.0 of PTB [4], at BESSY-II in Berlin, to measure the PSF of the MMs. This facility combines a narrow size beam (up to 7.5 × 7.5 mm^2), highly collimated (about 2 arcsec), and with a high photon density (about 10^{13} ph/s), to a precise mechanics, that moves the MM along the beam, providing sub-aperture exposures that need to be reconstructed via software analysis in the overall PSF.

Conventional X-ray sources are used at the PANTER facility of MPE near Munich [5]. To obtain a low divergence beam, the source is placed at large distance from the optic to be tested: in the case of PANTER, the source is at the end of a 120 m long vacuum tube. The residual divergence of the beam can be further reduced by a Fresnel Zone Plate designed for a specific wavelength. One for the 1.49 keV line is available at PANTER and was proven to provide a beam collimation of about 0.5 arcsec [6]. However, the large vacuum chamber of the PANTER facility does not allow a fast evacuation and venting, a key aspect when hundreds of MMs need to be characterized.

To overcome the limitations of the present facilities, INAF-OABrera have designed and realized a facility (Fig. 1) that creates a large parallel X-ray beam, covering the entire entrance pupil of the ATHENA MMs, in a small vacuum system capable to sustain the ATHENA telescope production at the rate of 2 MM/day. After the preliminary design in 2012 [7], the project became mature with the research led by INAF-OABrera [8-21], and the support of CNR-IMEM (Istituto dei Materiali per l'Elettronica e il Magnetismo, Parma-Italy), ESRF (European Synchrotron Radiation Facility, Grenoble-France), MPE (Max Planck Institute for Extraterrestrial Physics, Garching-Germany), DTU (Technical University of Denmark, Kongens Lyngby-Denmark), the European Space Agency (ESA) and several companies in charge of the different work packages [22]. The development and realization of BEaTriX was funded by ESA, AHEAD, ASI and internal INAF funds. Now, the facility is completed with the first beam line at the energy of 4.5 keV; a second beam line operating at 1.5 keV will be soon realized [23]. This paper reports the result of the commissioning and the first light at 4.5 keV with an ATHENA MM.

Figure 1. BEaTriX: view of the laboratory from the vacuum chamber containing the optical elements (left), and from the detector flanged at the end of the 12 m vacuum tube (right)

2. DESCRIPTION OF THE BEATRIX FACILITY

The working principle of BEaTriX is sketched in Fig. 2. As X-rays of 4.5 and 1.5 keV are absorbed in air, the beam is propagated in a vacuum system. The entire system is positioned on a stable foundation, designed and built to isolate the beam line from vibrations [11]. The compactness of the system (9×18 m^2) reduces the evacuation time with respect to bigger X-ray facilities.

X-rays at 4.5 keV are emitted by a microfocus source [19] with a Titanium anode (A in Fig.2), enclosed in a shielding box that avoid X-ray leaks in the operation environment. The source, with focal spot of 35×35 µm, is in UHV environment, separated by a 100 µm thick Be window. The flux of the Ti K_α doublet was measured to be 6×10^{11} ph/sec/sterad. The source is positioned in the focal point of a paraboloidal mirror (C in Fig.2). In this way, the rays, propagated through the vacuum tube (B in Fig.2), and reflected by the paraboloidal mirror, produce a collimated and parallel beam, with a horizontal size of 4 mm and a vertical size of 60 mm. The paraboloidal mirror was figured and polished at INAF-OAB [17,18]. The quality of the mirror was tested in X-rays at the PANTER X-ray facility, before and after coating at DTU with a bi-layer of Cr (4.6 nm) and Pt (30 nm). The result was in line with the simulations, giving an HEW of about 3 arcsec, as measured with the Fresnel Zone Plate in parallel beam configuration at 1.49 keV. Inside the BEaTriX facility, the mirror is mounted on two rotation stages to align it in pitch and yaw with respect to the X-ray source (Fig. 3), while the source is placed on a manipulator that assists the alignment of the source itself with respect to the paraboloidal mirror.

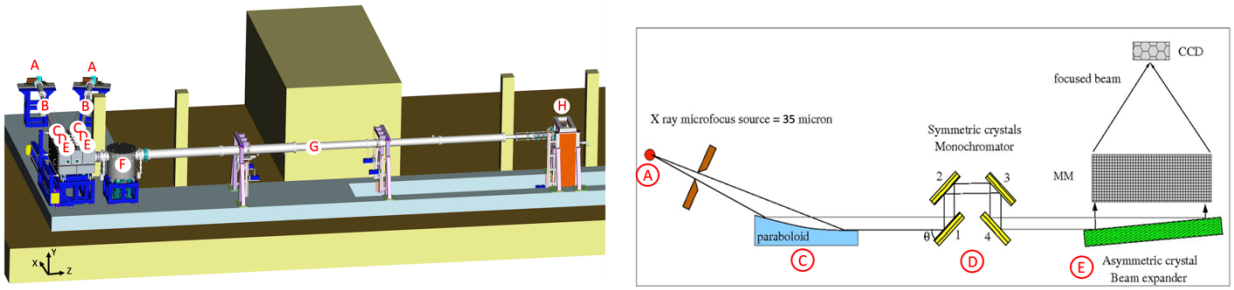

Figure 2. BEaTriX: layout (left), and optical design (right). The Athena coordinate system is also shown.

After the collimation, the beam is filtered tightly in energy with a 4-fold diffraction on silicon crystals (D in Fig.2), cut parallel to the (220) planes; two Channel Cut Crystals (CCC) are used to this goal (Fig. 3). Then, the beam is diffracted at about 90 deg by another silicon crystal (E in Fig. 2, called hereafter Beam Expander, or BE), asymmetrically cut with respect to the (220) planes, in order to ensure an expansion of about 50 times. This makes the final beam about the same size as the asymmetric crystal (170 mm × 60 mm). A beam expansion with an asymmetrically cut crystal was previously implemented at the Synchrotron Radiation Source at the Daresbury laboratory in UK, and was used for the calibrations of the SODART telescope for the Spectrum Röntgen Gamma satellite [24], reaching a beam divergence 10 times larger (~ 20 arcsec) than BEaTriX and expanding the beam in a single dimension.

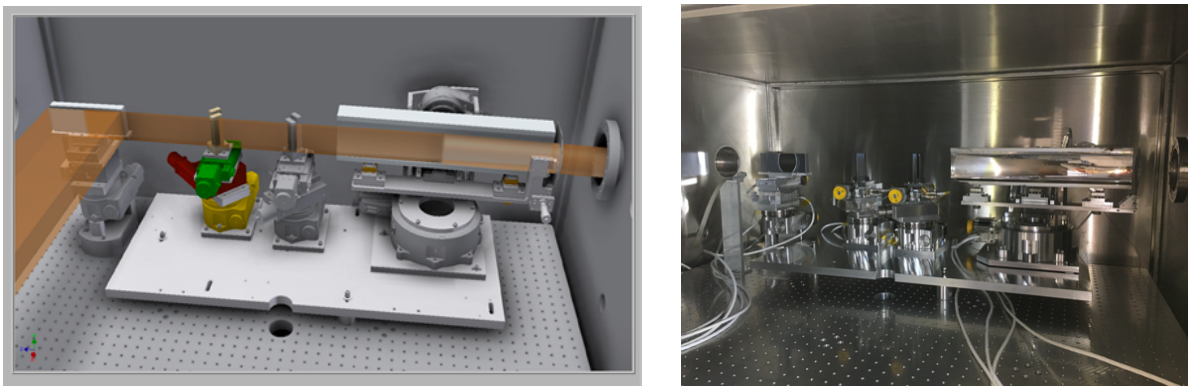

Figure 3. Design (left) and photo (right) of the components inside the Optical Chamber. From right: the paraboloidal mirror, the two CCCs in charge of the monochromation, the BE crystal in charge of the expansion. The Beam Monitor is visible in front of the BE.

The BEaTriX monochromator plays a key role in the horizontal beam collimation, due to the intrinsic dispersive power of asymmetrically-cut crystals [25]. Beside the 4-fold diffraction on symmetric crystals, a rotation of one Channel Cut Crystal (CCC) can be adopted to reduce the passing energy bandwidth. All the crystals are mounted on a set of three motors: a rotation stage for alignment in pitch, a cradle for alignment in roll and a linear stage to move the components in and out the X-ray beam (Fig. 3). The rotation of the second CCC can be obtained with the stage shown in yellow in Fig. 3 left. Using this possibility, BEaTriX can work with two configurations, one with "high flux – low collimation" (both CCCs aligned in pitch to the angle for maximum flux) and the second one with "low flux – high collimation" (second CCC rotated). The numerical values are hereafter given.
The beam collimation, stemming from the 35 µm source and the 3 arcsec HEW mirror, after a rotation of the second CCC of about 10 arcsec, was simulated to be HEW_{ver} = 1.0 arcsec and HEW_{hor} = 2.2 arcsec, in the vertical and horizontal direction respectively. These numbers are slightly degraded when including other sources of errors such as alignment, vibrations, temperature. All included, the collimation of BEaTriX in the two different configurations were simulated as follows:

- High flux – low collimation (CCC aligned at max flux)
  - Simulated flux = 60 ph/s/cm^2
  - Simulated collimation: HEW_{ver} = 1.46 arcsec, HEW_{hor} = 4.78 arcsec
- Low flux – high collimation (second CCC rotated by about 10 arcsec from the position of max flux)
  - Simulated flux = 10 ph/s/cm^2
  - Simulated collimation: HEW_{ver} = 1.46 arcsec, HEW_{hor} = 2.44 arcsec

The use of one or the other configuration is dictated by the quality of the optics to be tested.

The above mentioned components, the mirror and the crystals, are enclosed in the so called Optical Chamber (OC). In the same chamber, a Si-PIN detector (Fig. 3 right; Amptek, X123 with 25mm^2 area / 500 µm thickness / 25 µm Be window) is positioned in front of the asymmetric crystal, to monitor the flux stability and the stability of the aligned components. After generating a collimated expanded beam, we propagate it into the experimental chamber (F in Fig. 2), named Mirror Module Chamber (MMC), where the MMs are mounted and can be aligned by a hexapod (H-824.G2V by Physik Instrumente, red in Fig. 4 centre). The hexapod is mounted on a translational stage (blue in Fig. 4 centre), used to move the MM out of the beam, for the direct beam measurements. The MMs are installed, by means of 6 Neodymium magnets, on a titanium interface made by 3 parts, that can be adjusted to adapt to the width of the different MMs. The use of titanium and insulating washers, to fix the interface to the support connected to the hexapod, ensures a low conductive link from the alignment stage to the MM. Three PT100 sensors monitor the temperature of the bottom and top of the hexapod and the temperature at the MM level.

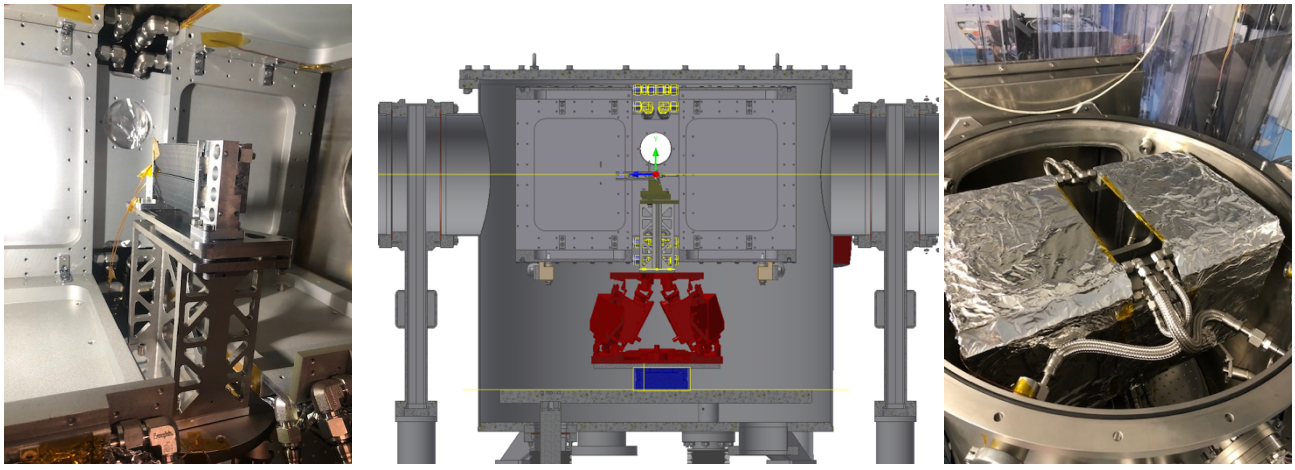

Figure 4. Left: MM mounted on its supporting structure, connected to the hexapod.
Centre: design of the MM Chamber, showing the thermal box (grey), the MM supporting structure in titanium (brown), the lightened truss in stainless-steel (grey), the hexapod (red) and the linear stage (blue).
Right: top view of the thermal box inside the MM Chamber, with the top cover removed for the installation of the thermal box

A thermal box (internal size: 350 mm × 350 mm × 600 mm) is also present to radiatively cool/heat the X-ray optics under test, in the temperature range T=293±25K. The chiller LAUDA PRO 245 E (T= -45 ÷200°C), the liquid Kryo 51 (T= -50 ÷120°C) and the design of the thermal box itself [13], enable the reaching of these and even larger temperature ranges. Two of the radiating panels are removable, giving accessibility to the MM and enabling possible temperature gradients of the MM in X and Y. Thermal gradient in Z direction can be possible by adding optional liquid lines: the current design is prepared for upgrade with 8 radiators in a very easy way, simply changing the connectors and adding more chillers.

The final path of the X-ray beam occurs in the 12 m vacuum tube (G in Fig. 2) that connect the MMC to the detector tower (H in Fig. 2), which hosts the detector and its motorizations (Fig. 1 right). The detector moves on three linear stages, whose travel ranges are: range-Z = 600 mm (for the focus search), range-Y = 1500 mm (for the vertical displacement of the focused image for MMs of different radii), and range-X = 200 mm (for the qualification of the beam). The detector is connected to the vacuum system by a bellow to enable the focus search. The 12 m long arm is made of 6 tubes to leave the possibility to modify in the future the focal length of the facility: major setup changes will be necessary but in principle focal distances other than 12 m are possible (f_{std} = 12000 ± 250 mm; $f_{possible\text{-}1}$ = 10295 ± 250 mm; $f_{possible\text{-}2}$ = 8295 ± 250 mm). The detector is an iKon-L from Andor, Model DW936R, mounting a 2048x2048 pixels (13.5 um × 13.5 um pixel size) back-illuminated sensor from E2V, model CCD42-40, in open configuration. A cold finger is present in front of the CCD sensor, to protect the sensor from possible condensation [19].

The vacuum system is divided into 4 modular compartments by gate valves, in order to operate the vacuum/venting independently. In particular, the MM Chamber can be isolated by two gate valves, for a fast MM replacement. The primary vacuum is accomplished by oil-free pre-vacuum and backing pumps, to avoid contamination of the optics. The primary pumps are placed outside the foundations (Fig. 1 left) to avoid vibrations. The 10^{-6} mbar vacuum is reached with magnetically levitated turbomolecular pumps: as they are flanged to the vacuum system, the magnetic levitation of the rotors was chosen to have low vibration operation. Vacuum sensors and electro-valves are available all along the beam line to monitor the vacuum status. Venting is performed with dried filtered air: the compressed air is filtered by a dedicated system and was certified to be in line with the BEaTriX requirement: particles comparable with ISO6 clean room, dew point lower than the operation temperature of the detector (-20°C), oil content < 0.015 mg/m^3. To allow the loading and unloading of the samples in a clean environment, the MM Chamber opens into an ISO5 clean tent [19].

Finally, the entire facility is driven with a LabVIEW software, entirely realized by INAF-OAB [21]. For some components it was sufficient to create the LabVIEW environment using the SDK provided by the suppliers; in other cases, ad-hoc codes were written. The implemented software solutions are described in another paper [21].

3. COMMISSIONING OF BEATRIX

3.1. The X-ray beam

The characterization of the X-ray beam was performed in size, collimation, intensity and uniformity. To reach the desired beam, a careful alignment procedure was developed and implemented (see [20]). The source was powered at 30kV/200μA, which was measured to produce 6.34×10^{11} ph/s/sr [19]. The collimation of the beam was qualified with a Hartmann plate specifically designed by OAB and produced with square holes of 400 μm, and pitch of 4 and 2 mm in the horizontal and vertical direction, respectively. The Hartmann plate was positioned on the support for the MM and installed in the MM Chamber. The light passing through the holes was collected by the CCD, with a slight intra-focal configuration to reduce the vignetting of the long tube. Since the beam is larger (170 mm × 60 mm) than the CCD sensor (27.6 mm × 27.6 mm), the CCD was moved in 21 positions, and the images were then stitched with software analysis. The mosaic was performed for the high-flux configuration. At each position, an image was taken cumulating photons for 30 min, and removing the background for an equivalent time. The total exposure of the mosaic lasted 21h. The light passing from each hole was analyzed to compute the centroid and the displacement with respect to the nominal position: this produced the image shown in Fig. 5 left which gives the low order contribution to the beam divergence. Cumulating the signal from all the holes, the intensity profiles was also compared to a convolution model to estimate the contribution to the divergence due to the imperfect spatial coherence of the beam (Fig. 5 right). More details can be found in [26].

Combining these results in quadrature, we have derived the divergence of the beam in the high-flux configuration, well in agreement with expectations:

$$HEW_{HOR\text{-}BEAM} = 3.45 \pm 0.25 \text{ arcsec}$$
$$HEW_{VER\text{-}BEAM} = 1.65 \pm 0.25 \text{ arcsec}$$

The intensity in this case was estimated as 50 ± 5 ph/s/cm^2, slightly lower than the expected 60 ph/s/cm^2. At present, we are working on increasing the flux with further optimization of the alignment, and preliminary results show the reaching of the expected 60 ph/s/cm^2.

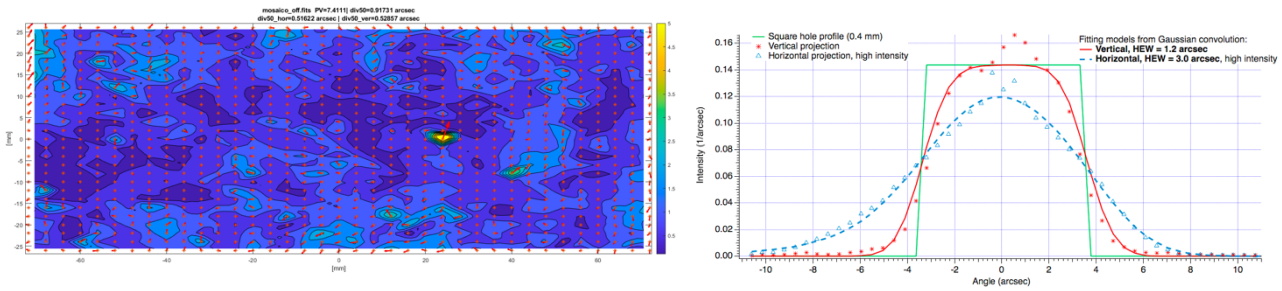

Figure 5. Left: composite mosaic of 3×7 CCD images, obtained in high-flux and low-collimation setup. Colours represent the amplitude of the divergence in arcsec and the red arrows the related direction. Right: Intensity profiles inside the holes.

The low flux – high collimation configuration was obtained rotating the second CCC by about 10 arcsec. In this case, the reduced flux cannot allow a mosaic of the beam; therefore, the beam was measured at the sole central position of the CCD. The exposure time was increase by a factor 4, for a total of 2 h. From the intensity profiles analysis, the contribution to the divergence due to the imperfect spatial coherence of the beam was reduced from 3.0 to 2.3 arcsec, well in line with the simulated 2.2 arcsec. On the assumption that we can combine in quadrature this result with the one obtained with the centroid method, we derived the divergence of the beam in the low-flux configuration:

$$HEW_{HOR\text{-}BEAM} = 2.7 \pm 0.25 \text{ arcsec}$$
$$HEW_{VER\text{-}BEAM} = 1.65 \pm 0.25 \text{ arcsec}$$

with an intensity estimated of 10 ph/s/cm^2. A confirmation of these data will be obtained as soon as a high-quality MM will be available, calibrated in other facilities.

For what concerns the uniformity of the beam, we have exposed a mosaic of the direct beam. The exposure time was 30 min per position, also in this case. The reconstructed image is shown in Fig. 6. The bottom left side of the beam is vignetted by the presence of the beam monitor, always present in the path but not affecting the qualification of the MM, as the beam is larger than needed for the ATHENA MMs. The same considerations apply to another minor vignetting, visible at the right side of the beam. The beam was measured as 168.4mm × 58.4mm, slightly smaller in height than the 60 mm of the MM. This is due to the height of the BE and the optical region of the parabolic mirror, both 60 mm as they were produced when the MM height was 54 mm. Possible improvements will be studied in the coming time.

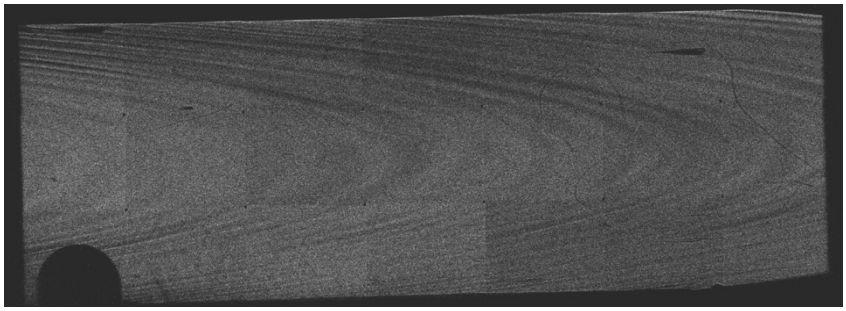

Figure 6. Intensity distribution of the X-ray beam, obtained from a mosaic of 3×7 images taken without the Hartmann plate. The vignetting on the lower left corner is due to the Beam Monitor present in front of the BE (Fig.3 right). The intensity difference among the CCD images is due to a background that could not be completely compensated.

The intensity distribution of the beam in Fig. 6 reproduces qualitatively the ray-tracing simulations obtained with the metrological data of the parabolic mirror: the pattern corresponds to the remaining surface errors of the mirror. We have removed this non-uniformity by implementing an oscillating movement (dithering) of the BE crystal, back and forth in Z-axis with a linear profile of the movement. The optimization is visible in Fig. 7 which compares the top left portion of the beam in case of no oscillation of the BE (left) and oscillations with range of 0.5 mm / period of 20 s (right). The oscillation was found not having significant impact on the beam collimation properties.

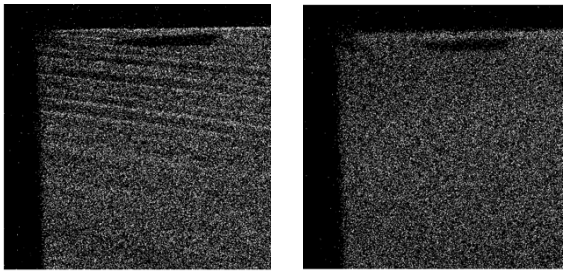

Figure 7. Improvement in the uniformity by dithering of the BE: no oscillation (left), oscillation with range = 0.5 mm and period = 20 s (right). The images are taken with exposure of 30min.

3.2. Throughput

BEaTriX was designed and realized as a vacuum system with 4 compartments (Short arm, Optical Chamber, MM Chamber, Long arm) separated by gate valves, where the MM Chamber is one of the sectors and can be isolated for a fast MM replacement. The entire system is limited in size and it was measured to be evacuated, from 1000 to 1×10^{-3} mbar, in 1h10min. Anyway, during operations, the sole MM Chamber needs to be evacuated: this is accomplished in about 30 min.

Regarding the alignment of the MM, a mechanical pre-alignment is performed at first in air; once in vacuum, the MM is aligned in pitch and yaw; finally, the focus search is performed. Concerning the exposure time, in the high flux configuration, 50 ph/s/cm^2 were measured. Considering a typical MM with Effective Area of 10 cm^2, and including the quantum efficiency of the CCD (60% at 4.5 keV), 10^5 ph are measured in about 6 min. With these numbers, a high test rate can be expected; the exact numbers will be clarified in the coming months when more tests will be performed.

3.3. Thermal system

The capacity of heating and cooling of the thermal system was tested by installing a mechanically representative MM in the MM Chamber (Fig. 4 left). One PT100 was attached to the MM brackets, and two thermocouples K-type were installed on the thermal box. Fig. 8 shows the heating (left) and cooling (right) curves. They show the reaching of T_{MM} = 63°C with the chiller at 90°C, and T_{MM} = -17°C with the chiller at -32°C, well beyond the required range of -5÷45 °C. In this test, the front door of the thermal box was kept open in the heating cycle, since the requirement could be easily satisfied also in this condition. The reaching of low temperatures instead required the front door of the thermal box to be closed.

The thermal box can also be used for acquisitions of the MM measurements at the accurate temperature of 20°C. Indeed, despite the isolation of the MM from the hexapod, a temperature of about 21.5°C was measured at the MM level, for hexapod temperature of about 25 °C. The MM was proven to be thermalized at 20°C by the use of the thermal box.

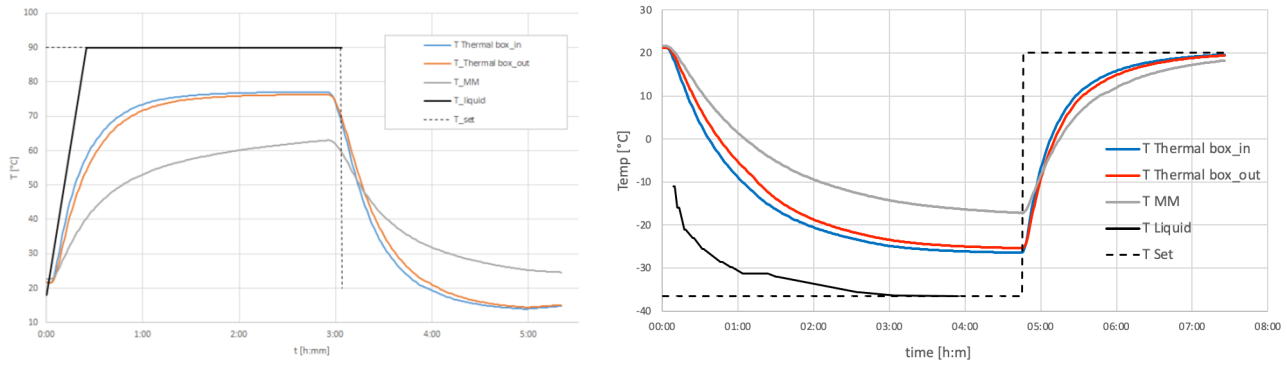

Figure 8. Use of the thermal box to test the MM at temperature different from 20°C (left: heating cycle, right: cooling cycle). The black line represents the chiller temperature; the grey line represents the MM, measured with a PT100 sensor; the red and blue lines are the temperature of the thermal box, measured with thermocouples K-type. The measurements show that a temperature range larger than the required -5÷45 °C can be reached.

.

4. FIRST LIGHT WITH A MM OF ATHENA

A first optically representative SPO mirror module (MM-0042) was measured in BeaTriX [26]. It consists of two identical XOUs, made of bare Si/SiO2 plates, with an on-axis incidence angle of about 0.3 deg, sufficiently small to reflect at 4.5 keV without the coating. The two XOUs are assembled in a parallel configuration; only the outer XOU was suitable for the measurement. Although this MM was produced in 2020 and is not representative of the present capability of SPO, it represents the first one available for measurements at 4.5 keV. The MM was mounted in the MM Chamber, and pre-aligned mechanically in air. The CCD was then moved in Y and positioned for collecting the X-rays deviated at the nominal angle ($4\times\theta_{inc}$). Pitch and yaw angles were optimized by maximizing the flux. A focus scan was then performed, searching for the minimum of the horizontal width of the image (Fig. 9 right), since the PSF is dominated by the vertical contribution and does not change significantly with focus variations.

The focused image was then integrated for 30min, to achieve about 10^5 photons, and the background subtracted. From the Encircled Energy plot, an HEW of 25.24 ± 0.89 arcsec was computed, in agreement with the value measured at BESSY. The direct beam was then measured, and the Effective Area was estimated as 6.84 ± 0.35 cm^2, to be compared to a theoretical value of 6.72 cm^2.

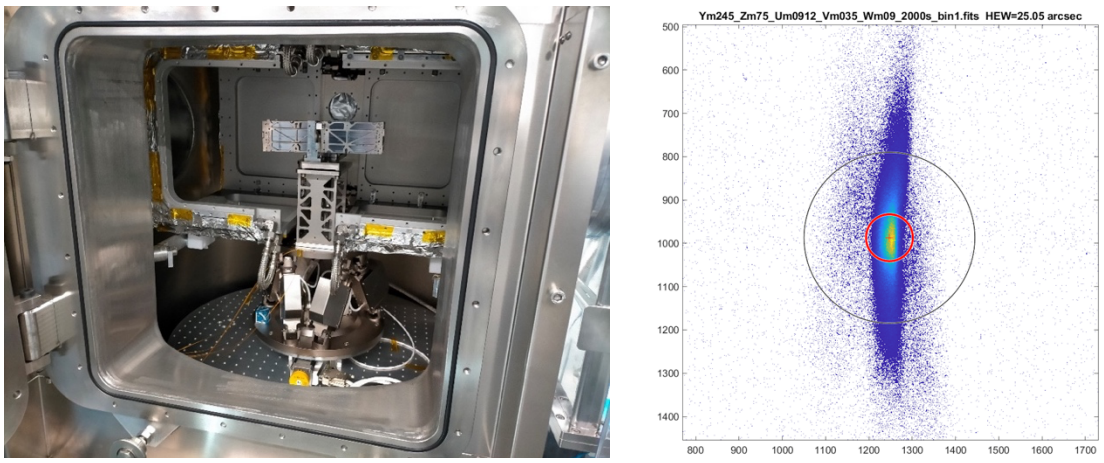

Figure 9. Left: MM-0042 installed in the experimental chamber of BEaTriX. Right: acquired image of MM-0042; the two circles correspond to HEW (red) and 90% EE (black).

5. CONCLUSIONS

The BEaTriX facility is now operative at the Merate premises of the INAF Astronomical Observatory of Brera. It provides a large collimated monochromatic beam at the energy of 4.5 keV, which enables the measurement of the ATHENA MMs, both for PSF and Effective Area. This paper has presented the commissioning results, proving the capabilities of this facility. The large collimated beam enables the illumination of the entire MM, with a sufficient flux. The small size of the vacuum facility enables a fast evacuation/venting time. These two aspects were proven to guarantee the capability for BEaTriX to follow the production of the SPO MMs at its rate of 2 MM/day. The beam was fully characterized. The capabilities to test the MM in the required temperature ranges was proven. An early prototype of SPO MM was measured in BEaTriX, showing the PSF and the Effective Area in line with the expectation.

The plan for the coming months, is to further qualify and possibly optimize the facility. A MM of higher quality, calibrated in other facilities, is expected by the end of 2022, and will permit the confirmation of the beam properties, by comparing the focused image to what expected from the beam reconstructed by the stitching procedure.

The second beam line, to operate at the energy of 1.5 keV, is being prepared. A study for a 6 keV beam line has also started. The work done for the 4.5 keV BEaTriX beam line has paved the way for a new accurate way to test X-ray optics.

ACKNOWLEDGMENTS

We acknowledge financial support from ESA (contract # 4000123152/18/NL/BW), AHEAD (grant #654215 and #871158), ASI (grant # 2019-27-HH.0) and INAF.

REFERENCES

[1] Nandra, K., Barret, D., Barcons, X., et al., "The Hot and Energetic Universe: A White Paper presenting the science theme motivating the Athena mission," http://arxiv.org/abs/1306.2307 (2013).
[2] Bavdaz, M., Wille, E., Ayre, M., et al., “The ATHENA X-ray optics development and accomodation”, Proc. SPIE 11852, 1185220 (2021)
[3] Collon, M. J., Babic, L., Barrière, N. M., et al. 2021, “X-ray mirror development and production for the ATHENA telescope”, Proc. SPIE 11852, 118521Z (2021)
[4] Handick, E., Cibik, L. Krumrey, M., “Upgrade of the X-ray parallel beam facility XPBF 2.0 for characterization of silicon pore optics”, Proc. SPIE 11444, 114444G (2020)
[5] Bradshaw, M., Burwitz, V, Hartner, G., et al., “Testing ATHENA optics: a new measurement standard at the PANTER x-ray test facility”, Proc. SPIE 11852, 1185223 (2021)
[6] Menz, B., Braig, C., Br auninger, H., et al., “Large area x-ray collimator—the zone plate approach”, Applied Optics Vol. 54, Issue 26, pp. 7851-7858 (2015)
[7] Spiga, D., Pareschi, G., Pelliciari, C., et al., “Functional tests of modular elements of segmented optics for x-ray telescopes via an expanded beam facility,” Proc. SPIE 8443, 84435F (2012)
[8] Spiga, D., Pelliciari, C., Bonnini, E., et al., "An expanded x-ray beam facility (BEaTriX) to test the modular elements of the ATHENA optics," Proc. SPIE 9144, 91445I (2014)
[9] Pelliciari, C., Spiga, D., Bonnini, E., et al., “BEaTriX, expanded soft x-ray beam facility for test of focusing optics, an update,” Proc. SPIE 9603, 96031P (2015)
[10] Spiga, D., Pelliciari, C., Salmaso, B., et al. “Design and advancement status of the Beam Expander Testing Xray facility (BEaTriX),” Proc. SPIE 9963, 996304 (2016)
[11] Salmaso, B., Spiga, D., Basso. S., et al., “Progress in the realization of the beam expander testing x-ray facility (BEaTriX) for testing ATHENA’s SPO modules,” Proc. SPIE 10699, 1069931 (2018)
[12] Spiga, D., Salmaso, B., Basso, S., et al, “Optical simulations for the laboratory-based expanded and collimated x-ray beam facility BEaTriX,” Proc. SPIE 11110, 111100E (2019)
[13] Basso, B., et al. Thermal simulations for characterization of ATHENA Mirror Modules with a radiating box in the BEaTriX facility, Proc. SPIE 111191, 111191I (2019)

[14] Salmaso, B., Spiga, D., Basso. S., et al., "BEaTriX (Beam Expander Testing X-ray facility) for testing ATHENA's SPO modules: advancement status," Proc. SPIE International Conference on Space Optics 2018, Vol. 11180, 1118026 (2019)
[15] Salmaso, B., et al. BEaTriX, the Beam Expander Testing X-ray facility for testing ATHENAs SPO modules: progress in the realisation, Proc. SPIE 11119, 111190N (2019)
[16] Ferrari, C., Beretta, S., Salmaso, B.,et al., "Characterization of ADP crystals for soft x-ray optics of the Beam Expander Testing X-ray facility (BEaTriX)," Journal of Applied Crystallography, 52, 599-604 (2019)
[17] Spiga D., Salmaso, B., Basso, S., et al., "Performance simulations for the ground-based, expanded-beam X-ray source BEaTriX", Proc. SPIE 11837, 118370O (2021)
[18] Vecchi, G., Cotroneo, V., Ghigo, M., et al., Manufacturing and testing of the X-ray collimating mirror for the BEaTriX facility, Proc. SPIE 11822, 118220N (2021)
[19] Salmaso, B., Basso, S, Cotroneo, V. et al. "Building the BEaTriX facility for the ATHENA mirror modules X-ray testing", Proc. SPIE 11822, 118220M (2021)
[20] Basso, S., Salmaso, B., Ghigo, M., et al.,"The expanded, parallel and monochromatic X-ray beam of BEaTriX: alignment and characterization", Proc. SPIE this conference
[21] Ghigo, M., Salmaso, B., Basso, S., et al., "The control software of the BEaTriX X-ray beam calibration facility: problems and solutions", Proc. SPIE this conference
[22] http://www.brera.inaf.it/beatrix-facility/
[23] Spiga, D., Salmaso, B., Basso, S., et al., "Optical design and performance simulations for the 1.49 keV beamline of the BEaTriX X-ray facility", Proc. SPIE ICSO 2022
[24] Christensen, F., Hornstrup, A., Frederiksen, P., et al., "Expanded beam x-ray optics calibration facility at the Daresbury Synchrotron," Proc. SPIE 2011, 540 (1994)
[25] Sanchez del Rio, M., Cerrina, F., "Asymmetrically cut crystals for synchrotron radiation monochromators", Review of Scientific Instruments 63, 936 (1992)
[26] Basso, S., Salmaso, B., Spiga, D., et al., "First light of BEaTriX, the new testing facility for the modular X-ray optics of the ATHENA mission", accepted for publication on Astronomy and Astrophysics (2022)